Supplementary

Robust Synthesis of Free-Standing and Thickness Controllable Conjugated Microporous Polymers Nanofilms

Zhen Chen, Min Chen, Yanlei Yu and Limin Wu*

1. Materials

All materials were used as received without further purification. Copper(I) iodide (≥99.5%), triphenylphosphine (≥99.0%), 1,4-diiodobenzene (≥98.0%), tris(4-iodophenyl)amine (≥98.0%), triethylamine (≥99.5%), 1,3,5-tribromobenzene (≥98.0%) and trimethylsilylacetylene (≥98.0%) were purchased from Aladdin Chemical Reagent Co., Ltd. (China). 4,4'-Diiodobiphenyl (≥98.0%), 1,4-diaminobenzene (≥99.0%) and tris(4-iodophenyl)amine (≥98.0%) were purchased from J&K Chemical CO., Ltd. (China). Xylene (AR), acetonitrile (AR), ethanol (≥99.7%) and potassium carbonate (≥99.0%) were purchased from Sinopharm Chemical Reagent Co., Ltd. (China). 1,3,5-Triformylbenzene (97.0%) was purchased from Sigma-Aldrich Co., LLC.. Tetraphenylethylene (98.0%) was purchased from Alfa Aesar Chemical Co., Ltd.. bis(triphenylphosphine)palladium(II) dichloride (Pd, 15.2%) was purchased from Adamas Reagent Co., Ltd.(China).

2. Synthesis methods

Synthesis of 1,3,5-[(trimethylsilyl)ethynyl]benzene:

1,3,5-Tribromobenzene (4.84 g, 15.35 mmol), $Pd(PPh_3)_2Cl_2$ (0.2 g, 0.285 mmol) and CuI (0.025 g, 0.13 mmol) were dissolved in 150 mL degassed tolune and 50 mL degassed Et_3N, the above mixture was added into a 250 mL three-necked flask, then

(trimethylsilyl)acetylene (5.43 g, 55.3 mmol) was dropwise added into the mixture under N_2. The reaction mixture was stirred at 80°C for 24 h under N_2. After cooled to room temperature, the solid was filtered and washed with diethyl ether. The solvent was removed in vacuum and the residue was purified by flash chromatography on silica gel (hexanes) to afford 1,3,5-[(trimethylsilyl)ethynyl]benzene (5.3g, 93.4%).

^{1}H NMR ($CDCl_3$, 400 MHz): δ= 7.49 (s, 3H), 0.24 (s, 27H) ppm. IR (KBr): ν = 2959, 2899, 2163, 1579, 1411, 1251, 844, 760, 700, 679 cm^{-1}.

Synthesis of 1,3,5-triethynylbenzene (TEB):

1,3,5-[(Trimethylsilyl)ethynyl]benzene (6.25 g, 30 mmol) was dissolved in 100 mL methanol, potassium carbonate (12.45 g, 90 mmol) was added to the solution. The reaction mixture was stirred at room temperature for 6 h before poured into water. The aqueous layer was extracted with dichloromethane then the solvent was removed in vacuum and the residue was purified by flash chromatography on silica gel (petroleum ether) to afford TEB (4.0 g, 96%).

^{1}H NMR ($CDCl_3$, 400 MHz): δ = 7.57 (s, 3H), 3.11 (s, 3H) ppm. ^{13}C NMR ($CDCl_3$, 400 MHz,): δ = 135.64, 122.92, 81.60, 78.68 ppm. IR (KBr): ν = 3278, 3061, 2109, 1787, 1578, 1412, 1259, 930, 883, 670 cm^{-1}.

Synthesis of tetra(p-iodophenyl)ethylene (TIPE):

Tetraphenylethylene (0.22 g, 0.66 mmol), I_2 (0.46 g, 1.60 mmol) and $PhI(OAc)_2$ (0.62 g, 1.60 mmol) were dissolved in dry $CHCl_3$ (15 mL), and stirred at room temperature in the dark for 72 h. The solid was filtered and washed with petroleum ether. The residue was recrystallized from dichloromethane to afford TIPE (0.43g, 78%).

^{1}H NMR ($CDCl_3$, 400MHz): δ = 7.47 (d, J = 8.4 Hz, 8 H), 6.71 (d, J = 8.4 Hz, 8 H) ppm. ^{13}C NMR ($CDCl_3$, 400MHz): δ = 142.0, 139.8, 137.2, 133.0, 93.0 ppm. IR (KBr): ν = 1575, 1479, 1385, 1099, 1054, 1003, 863, 823, 783, 723, 621 cm^{-1}.

Synthesis of CMP1-4 and Imine-CMP powders

CMP1-4 powders were synthesized according to the previous literature[s1]. Imine-CMP powder was synthesized according to a modified procedure as follows: 1,3,5-triformylbenzene (24 mg, 0.15 mmol) and 1,4-diaminobenzene (24 mg, 0.225 mmol) were dissolved in the mixture of xylene (10 mL) and acetic acid (1.0 mL), then degassed by three evacuate-refill cycles and stirred at 90 °C for 24 h under a nitrogen atmosphere. The precipitate was collected by filtration and washed three times with water, chloroform, and acetone and then further washed by Soxhlet extractions for 24 h with dichloromethane, methanol and THF, respectively. The product was dried under vacuum at 90 °C for 24 h. (Yield, 80 %).

Synthesis of CMP nanofilms by oil-water interfacial polymerization from Sonogashira-Hagihara reaction: Typically, an aqueous phase consisting of Et_3N (20 mL) and CuI (1.5 mmol%) in 40 mL water was first charged into a 250 mL three-necked round-bottomed flask and degassed by three evacuate-refill cycles under N_2. Then an organic phase consisting of 1,3,5-triethynylbenzene (TEB) (0.35 mM), with 1,4-diiodobenzene (DIB) (0.5 mM), or 4,4'-diiodobiphenyl (0.5 mM), or tris(4-iodophenyl)amine(TIPA) (0.35 mM), or tetra(p-iodophenyl)ethylene (TIPE) (0.26 mM), and $Pd(PPh_3)_2Cl_2$ (1.5 mmol%) in 40 mL xylene was slowly added into the above three-necked round-bottomed flask, and degassed by three evacuate-refill cycles under N_2, and heated to 70^{o}C. These mixtures were held still at that temperature without any stirring for 24 h under a nitrogen atmosphere. The films formed at the oil-water interface were transferred to an ethyl acetate reservoir to rinse the unreacted monomers from the surfaces and denoted as CMP-1-nanofilm, CMP-2-nanofilm, CMP-3-nanofilm and CMP-4-nanofilm, respectively.

Synthesis of Imine-CMP-nanofilm by oil-water interfacial polymerization from

Schiff-base reaction: An aqueous phase consisting of acetic acid (1.0 mL) in 40 mL water was charged into a 250 mL three-necked round-bottomed flask and degassed by three evacuate-refill cycles under N_2. Then an organic phase consisting of 1,3,5-triformylbenzene (TFB) (0.66 mM) and 1,4-diaminobenzene (DAB) (0.99 mM) in 40 mL xylene was added into the above three-necked round-bottomed flask slowly. This mixture was degassed by three evacuate-refill cycles under N_2, and heated to 90 ^oC and held still at that temperature without any stirring for 72 h under a nitrogen atmosphere. The film formed at the oil-water interface was transferred to an ethyl acetate reservoir to rinse unreacted monomers from the surface.

3. Characterization

FT-IR spectra were recorded on a Nicolet Nexus 470 spectrometer using spectroscopic grade KBr. ^1H and ^{13}C NMR measurements were recorded with a Bruker Advance 400 spectrometer, and chemical shifts (δ in ppm) were determined with a residual proton of the solvent as standard. Solid-State ^{13}C CP/MAS NMR spectra were recorded on Bruker AVANCE III 400 WB spectrometer at ambient temperature with a magic angle spinning rate of 12.0 kHz. Powder X-ray diffraction patterns were recorded on D8 ADVANCE X-Ray Diffractometer. UV−Vis absorption spectra were recorded at room temperature on the Hitachi U-4100 UV-Vis spectrophotometer. Energy dispersive X-ray absorption spectroscopy (EDS) analysis and Field-emission scanning electron microscopy (FE-SEM) measurements were conducted on Carl Zeiss Ultra 55 equipped with an Oxford energy dispersive X-ray system. High-resolution transmission electron microscopy (HR-TEM) measurements were performed on FEI Tecnai G2 F20 S-Twin. Atomic force microscopy (AFM) measurements were performed on Bruker MultiMode 8 microscope under a tapping mode and ambient conditions. Kr sorption isotherm measurements were conducted on Quantachrome Autosorb-iQ3-XR, the mass of CMP-

1-4- and Imine-CMP-nanofilms used in this measurement were 11.4 mg, 6.3 mg, 11.4 mg, 7.5 mg and 2.8 mg, respectively. N_2 sorption isotherm measurements were conducted on Quantachrome Autosorb-iQ, the mass of CMP-1-4 and Imine-CMP bulk powders used in this measurement were 135 mg, 106 mg, 102 mg, 91 mg and 71 mg, respectively. UV–Vis transmission spectra were recorded on the Hitachi U-4100 UV-Vis spectrophotometer (nanofilms were coated on glass plate, thicknesses are around 130 nm). Water contact angle (WCA) of nanofilm was characterized by OCA15 contact angle analyzer (Dataphysics, Germany) averaged over 3 fresh spots using 3 μL deionized water. Fluorescence experiments were carried out on PTI QM40 Fluorescence Lifetime Spectrometers, the CMP nanofilm was first adhered to one side of quartz plate (0.9*4.0 cm) and then put into a quartz cuvette (1.0*1.0*4.0 cm) filled with 3 mL acetonitrile, the corrected fluorescence spectra were recorded after the addition of small aliquots of nitroaromatic solution (30 mM) into the quartz cuvette [S2].

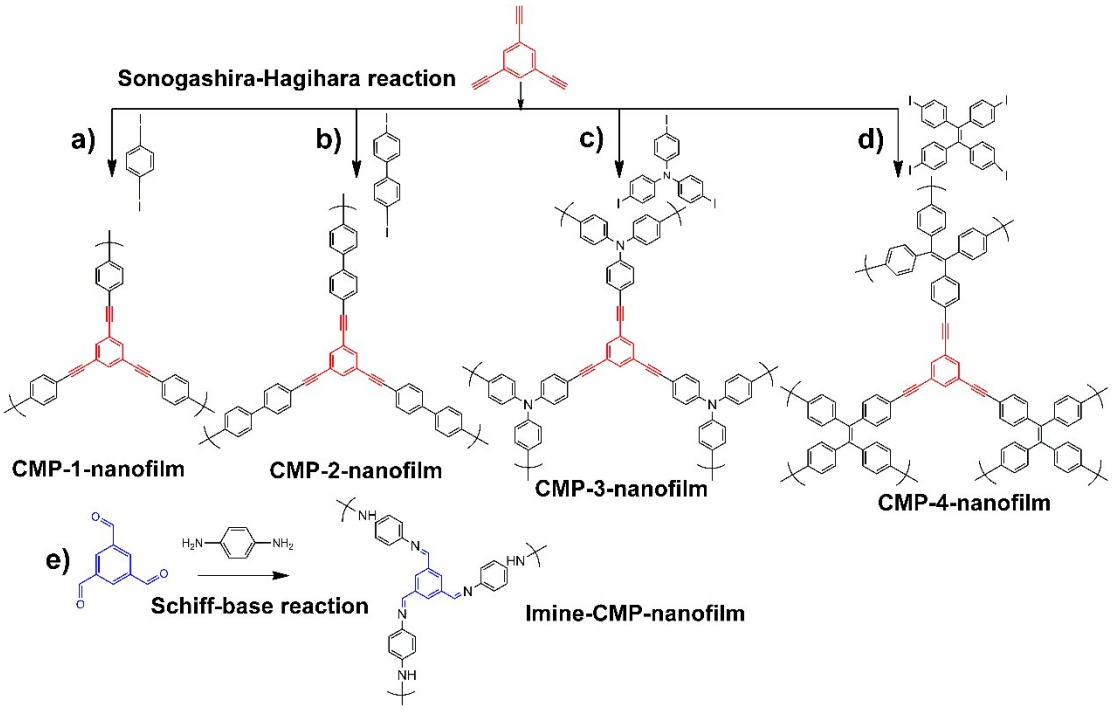

Figure S1. (a-e) Syntheses of CMP-1- to CMP-4 nanofilms and Imine-CMP-nanofilm. Through 1,3,5-triethynylbenzene with (a) 1,4-diiodobenzene, (b) 4,4'-diiodobiphenyl, (c) tris(4-iodophenyl)amine and (d) tetra(p-iodophenyl)ethylene; or (e) 1,3,5-triformylbenzene with 1,4-diaminobenzene.

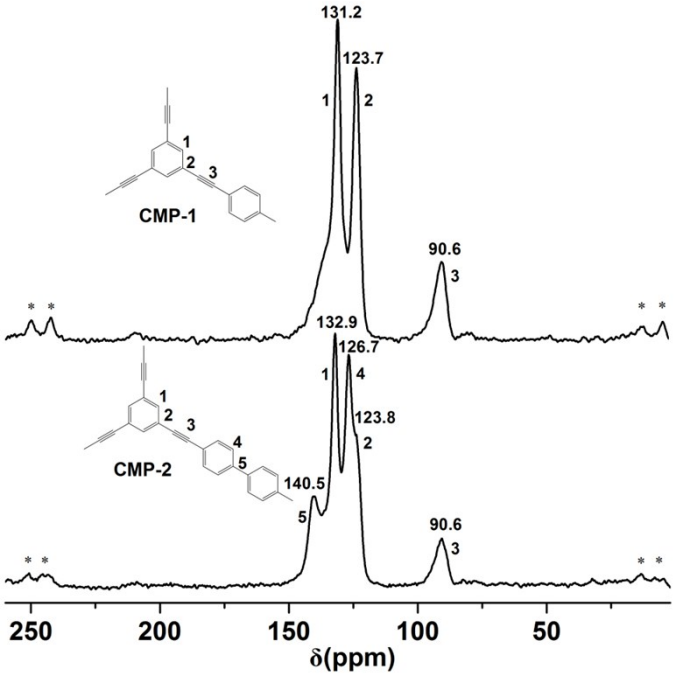

Figure S2. Solid-state ^{13}C CP/MAS NMR spectra of CMP-1 and CMP-2 powders (signals with asterisks are rotational sidebands).

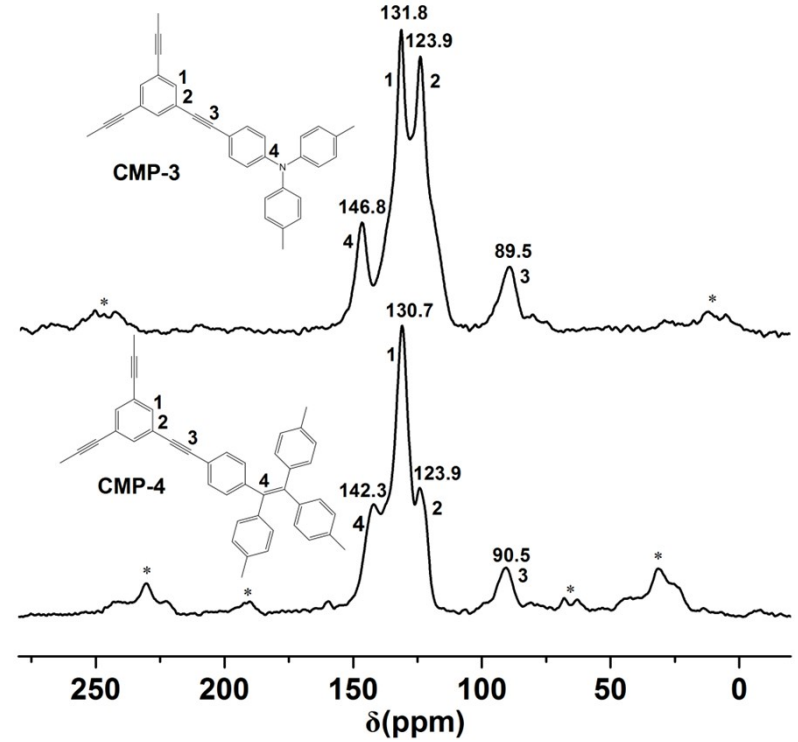

Figure S3. Solid-state ^{13}C CP/MAS NMR spectra of CMP-3 and CMP-4 powders (signals with asterisks are rotational sidebands).

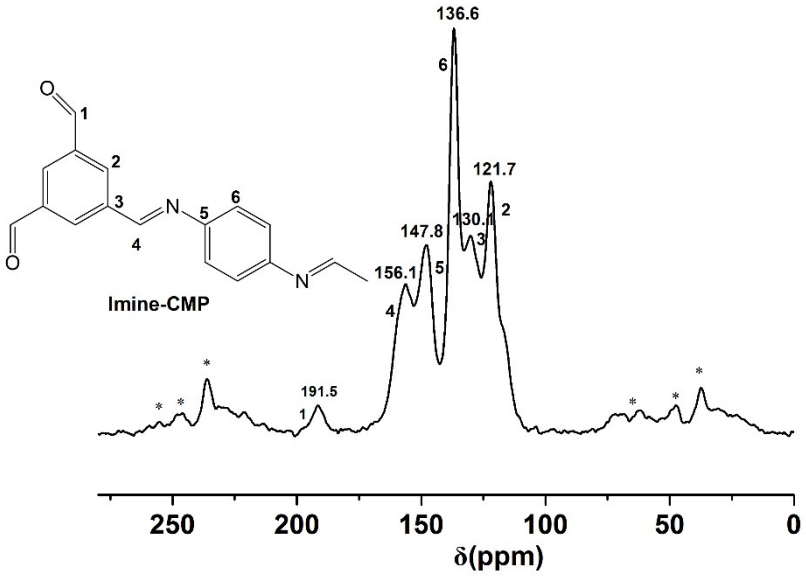

Figure S4. Solid-state ^{13}C CP/MAS NMR spectra of Imine-CMP powders (signals with asterisks are rotational sidebands).

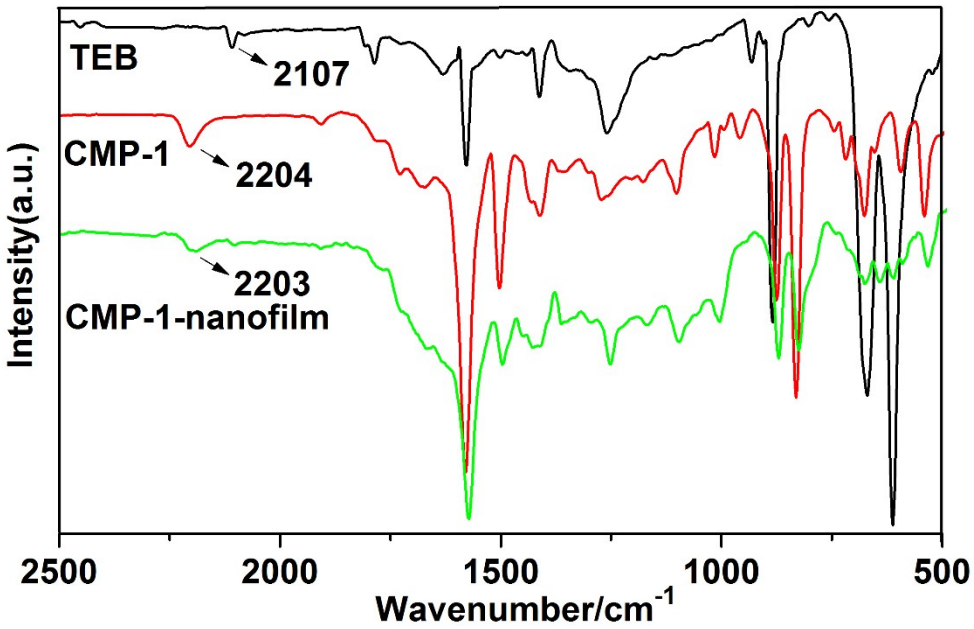

Figure S5. FT-IR spectra of TEB, CMP-1 powder and CMP-1-nanofilm.

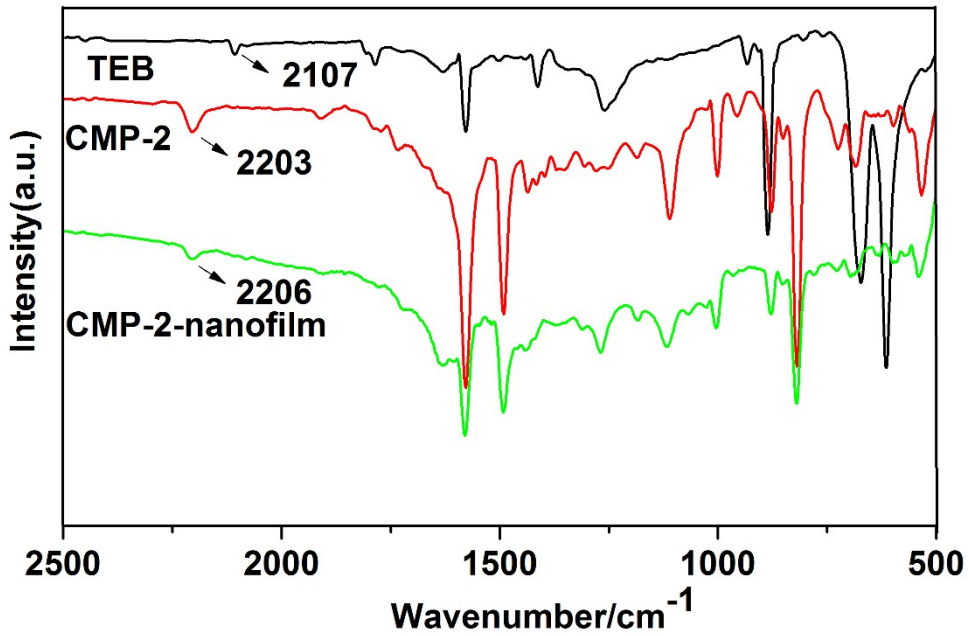

Figure S6. FT-IR spectra of TEB, CMP-2 powder and CMP-2-nanofilm.

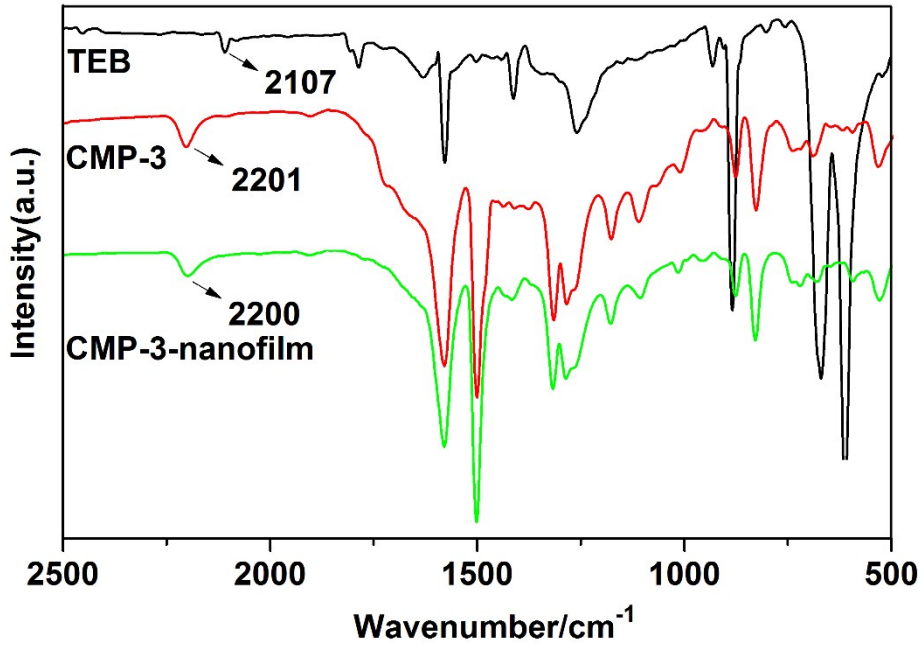

Figure S7. FT-IR spectra of TEB, CMP-3 powder and CMP-3-nanofilm.

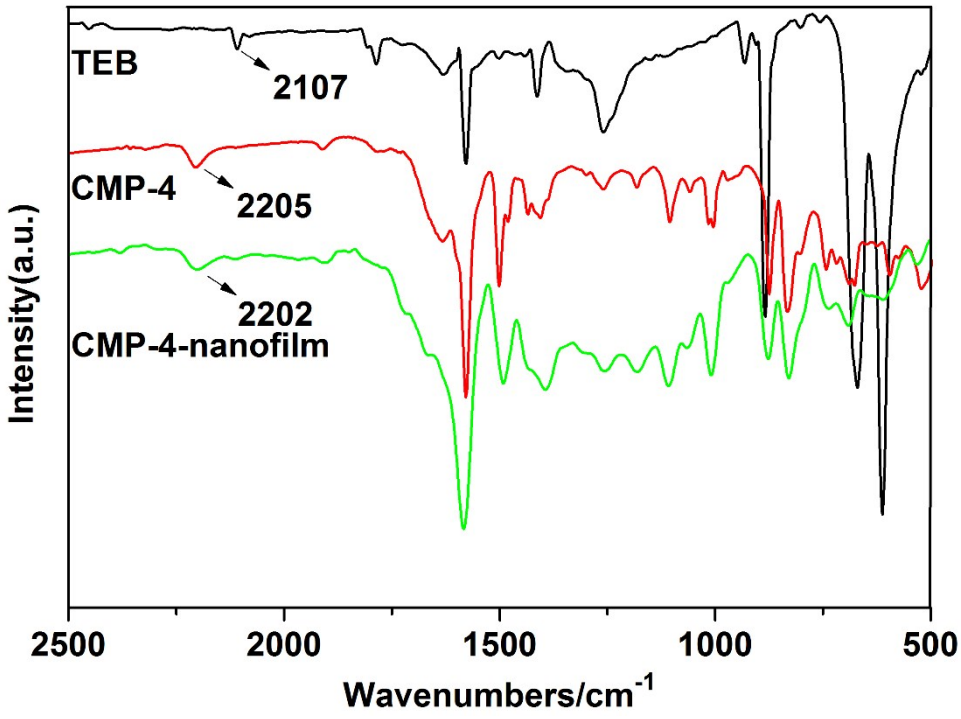

Figure S8. FT-IR spectra of TEB, CMP-4 powder and CMP-4-nanofilm.

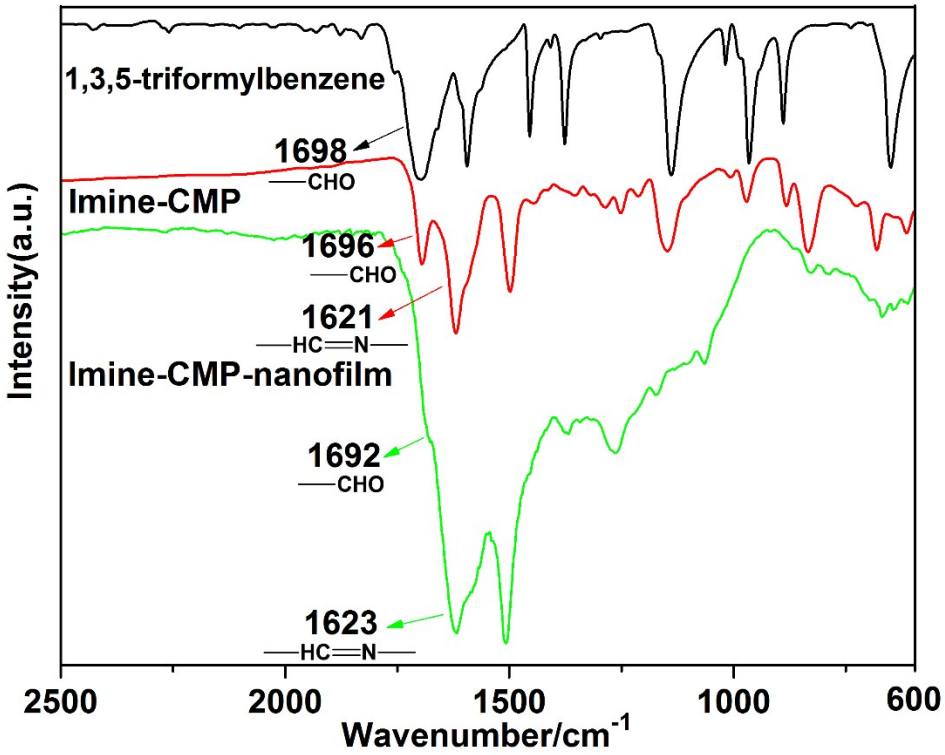

Figure S9. FT-IR spectra of TFB, Imine-CMP powder and Imine-CMP-nanofilm.

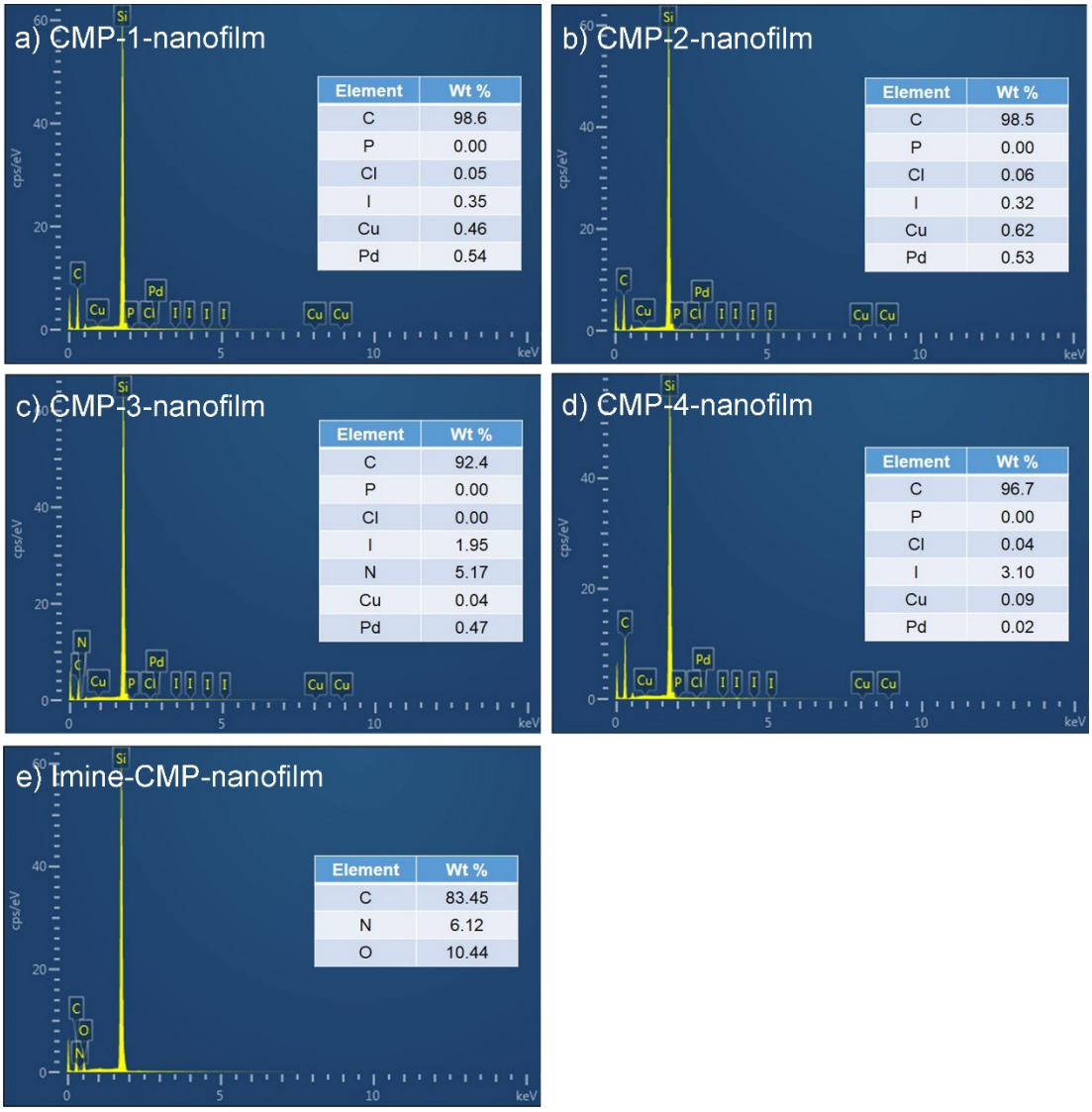

Figure S10. EDS sum spectra of CMP nanofilms, inserts show quantification in wt. %. A small amount of iodine element in CMP-1-4 nanofilms and a considerable amount of oxygen element in Imine-CMP-nanofilm can be attributed to the residual terminal iodine and aldehyde in the structure of monomers. The high silicon content can be ascribed to the silicon wafer (in EDS measurements, all of nanofilms were coated on the silicon wafer).

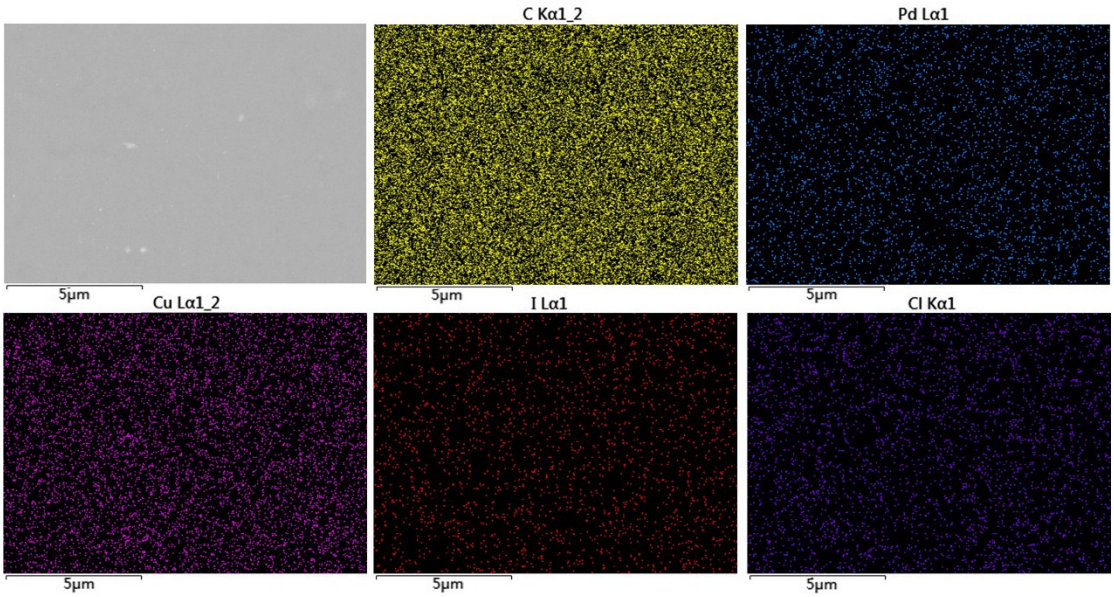

Figure S11. EDS element maps of CMP-1-nanofilm. There is no any large, aggregated Pd and Cu species in the nanofilm.

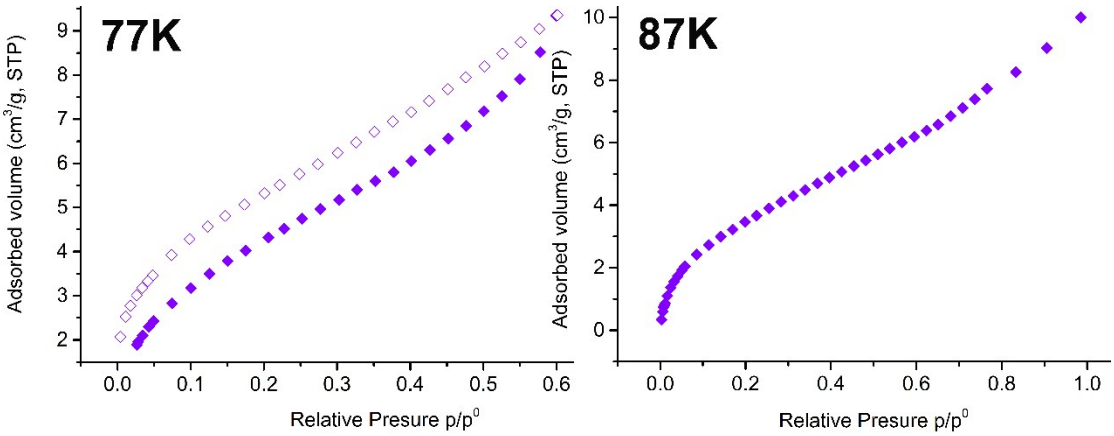

Figure S12. a) Kr sorption isotherms for Imine-CMP-nanofilm measured at 77 K (solid rhombuses: adsorption, open rhombuses: desorption). b) Kr sorption isotherm for the Imine-CMP-nanofilm measured at 87 K (solid rhombuses: adsorption).

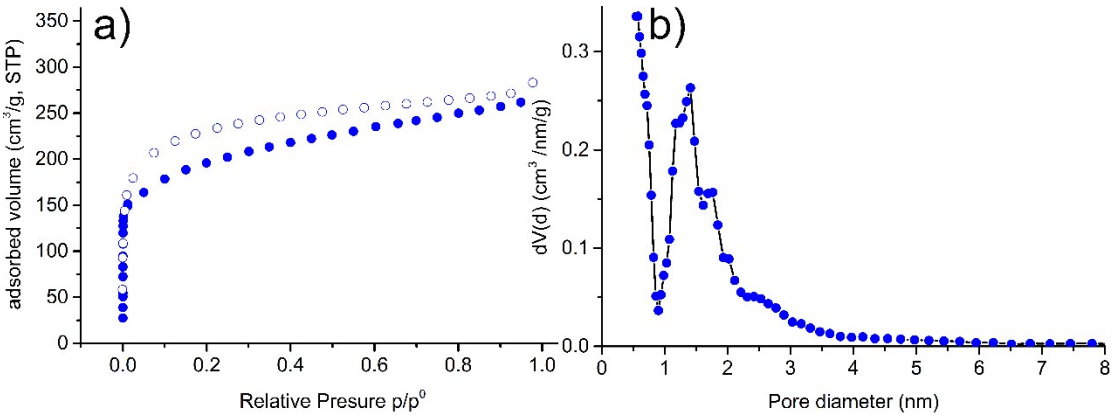

Figure S13. a) N_2 sorption isotherms for CMP-1 powder measured at 77 K (solid circles: adsorption, open circles: desorption). b) Pore size distribution profile of CMP-1 powder.

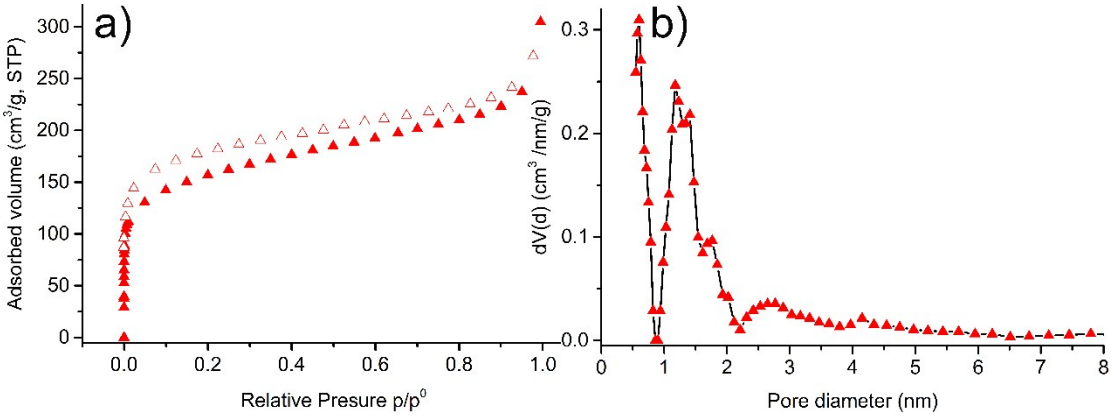

Figure S14. a) N_2 sorption isotherms for CMP-2 powder measured at 77 K (solid circles: adsorption, open circles: desorption). b) Pore size distribution profile of CMP-2 powder.

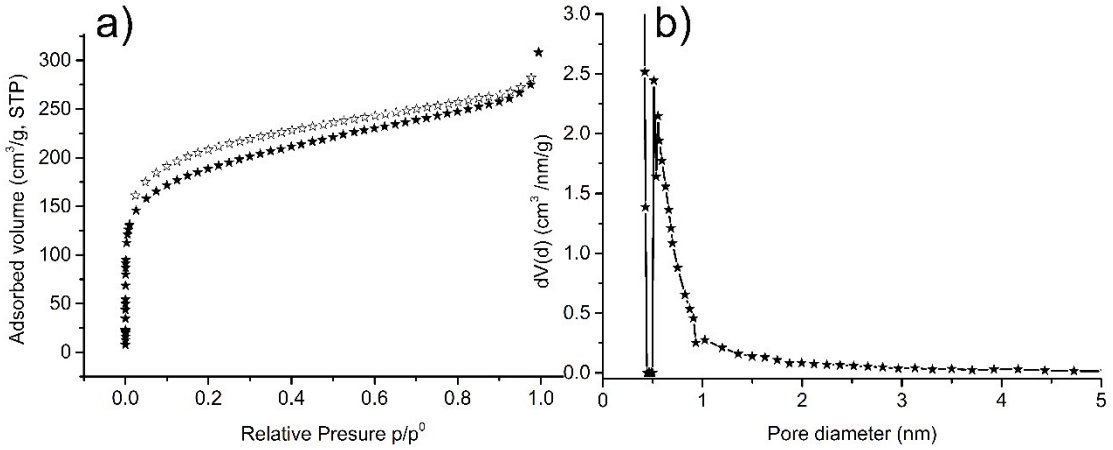

Figure S15. a) N_2 sorption isotherms for CMP-3 powder measured at 77 K (solid circles: adsorption, open circles: desorption). b) Pore size distribution profile of CMP-3 powder.

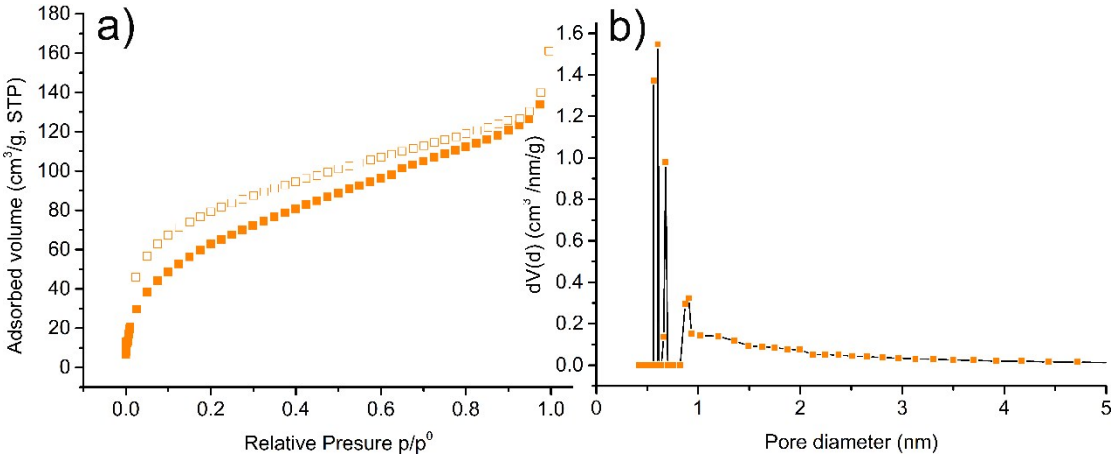

Figure S16. a) N_2 sorption isotherms for CMP-4 powder measured at 77 K (solid circles: adsorption, open circles: desorption). b) Pore size distribution profile of CMP-4 powder.

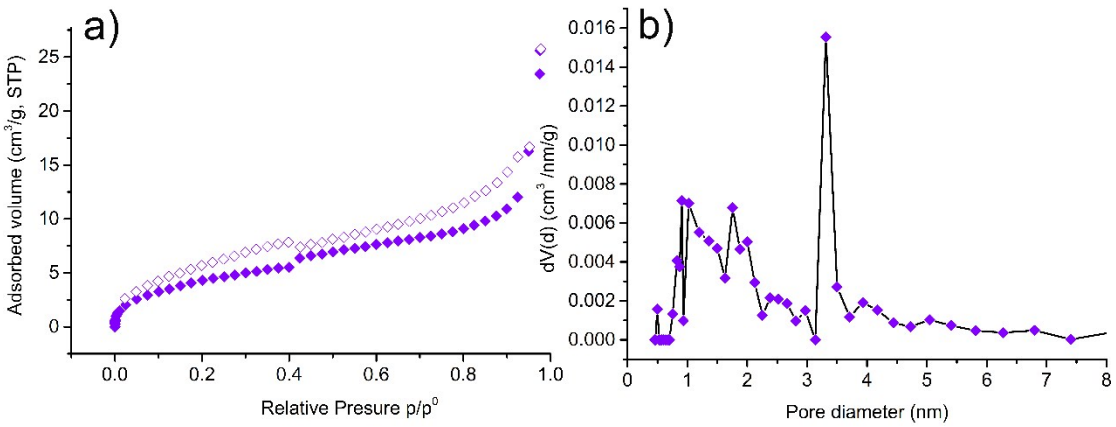

Figure S17. a) N_2 sorption isotherms for Imine-CMP powder measured at 77 K (solid circles: adsorption, open circles: desorption). b) Pore size distribution profile of Imine-CMP powder.

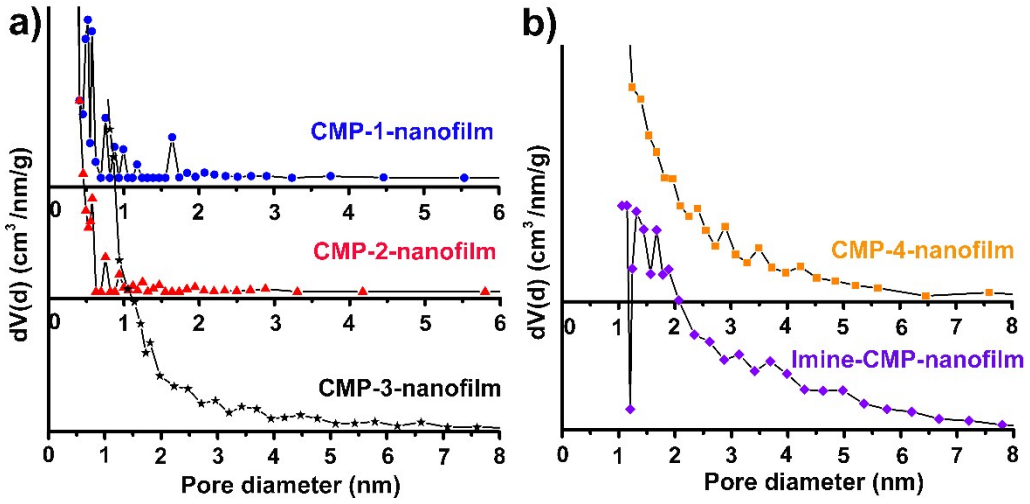

Figure S18. a-b) Pore size distribution profiles of CMP nanofilms.

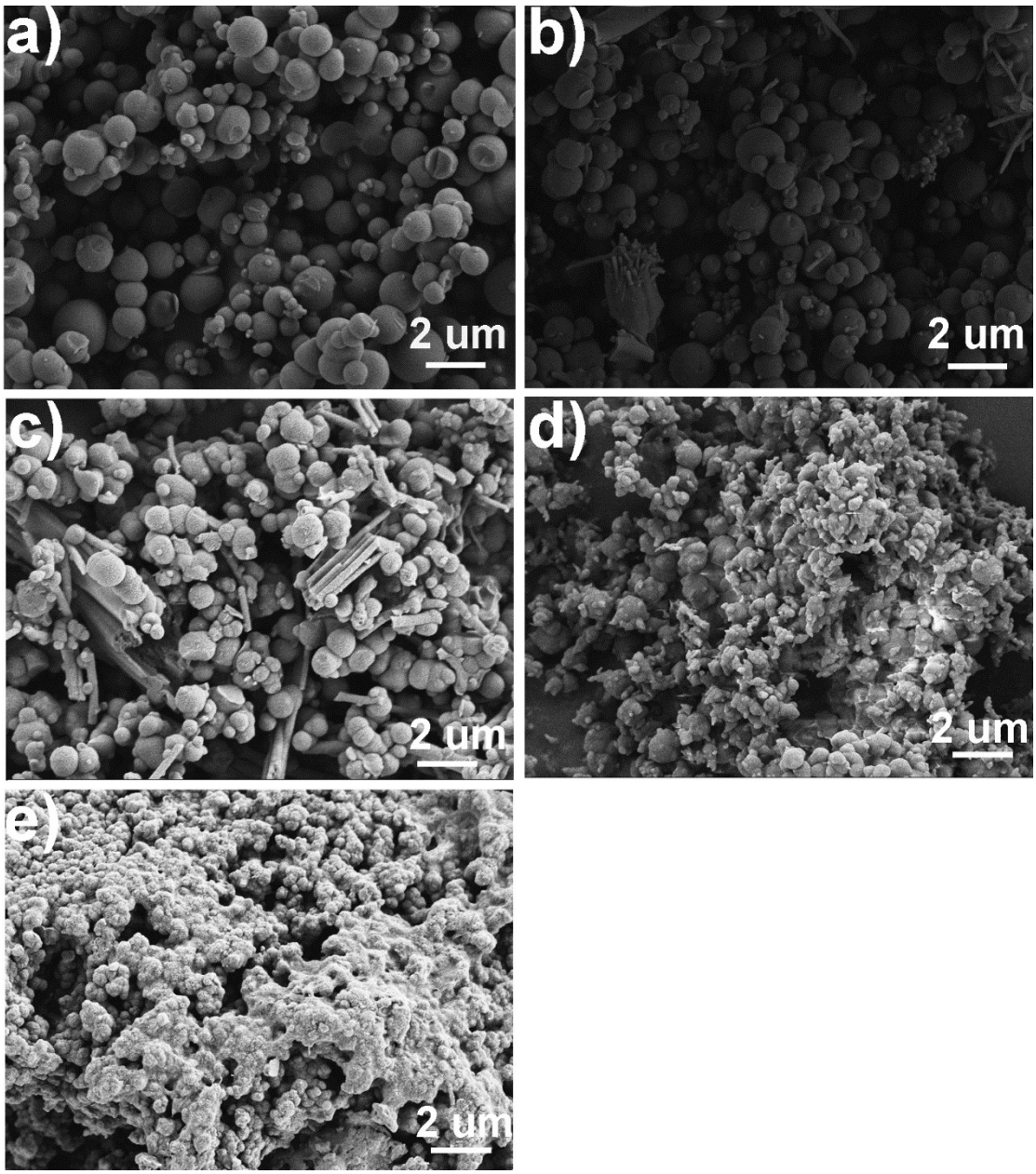

Figure S19. SEM images of CMP-1-4 and Imine-CMP powders. a) CMP-1 powders. b) CMP-2 powders. c) CMP-3 powders. d) CMP-4 powders. e) Imine-CMP powders.

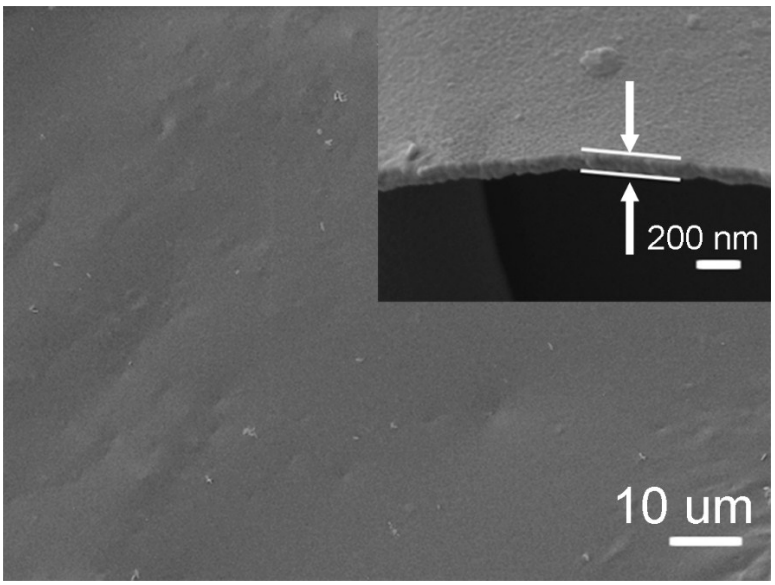

Figure S20. Surface SEM image of Imine-CMP nanofilm, insert: cross section of nanofilm.

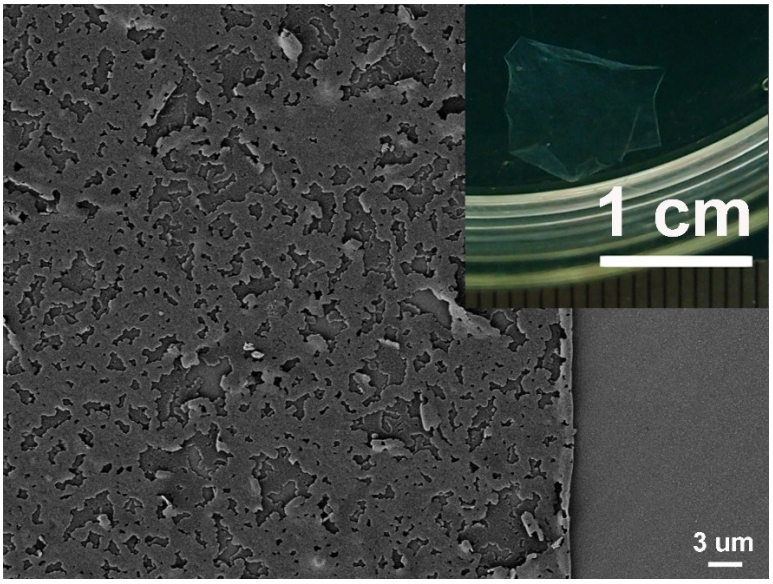

Figure S21. FE-SEM image of the CMP-1-nanofilm (thickness is around 30 nm). The inset is optical image of the nanofilm immersed in the ethanol phase. The holes and cracks can be seen in the thinner nanofilms, probably because that the monomer concentrations is too low at the phase boundary to form homogeneous nanofilms.

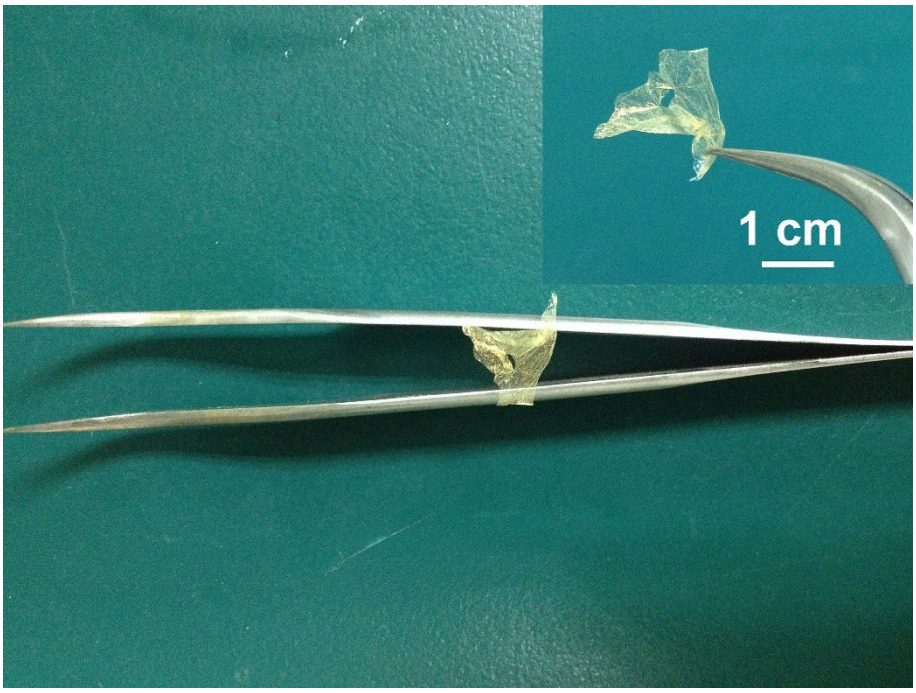

Figure S22. Photo images of the free-standing CMP-1-nanofilm.

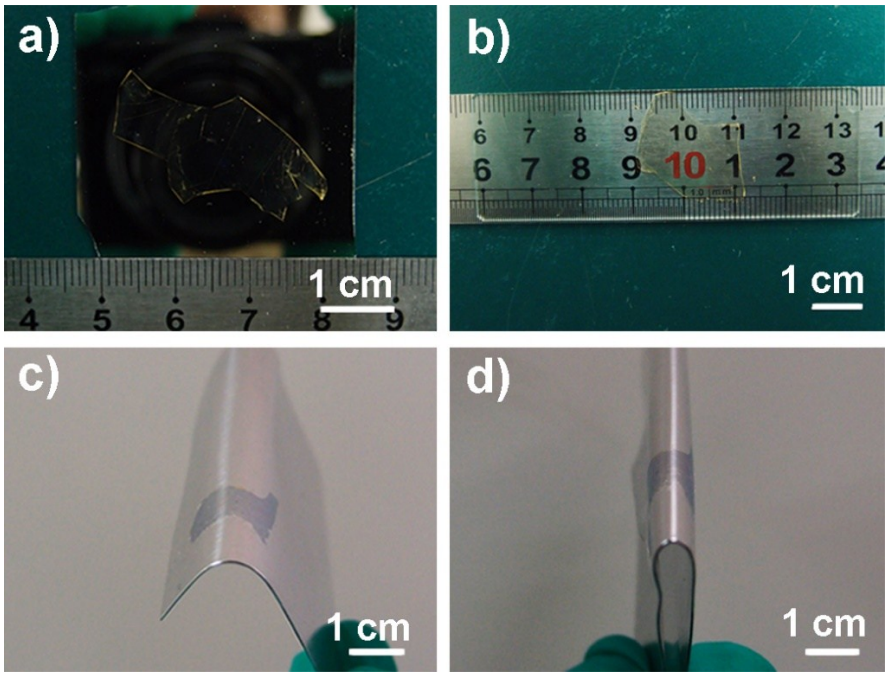

Figure S23. Photo images of CMP-1-nanofilm. a) On silicon wafer plate. b) On quartz plate. c) On aluminum flake. d) The bending status of c).

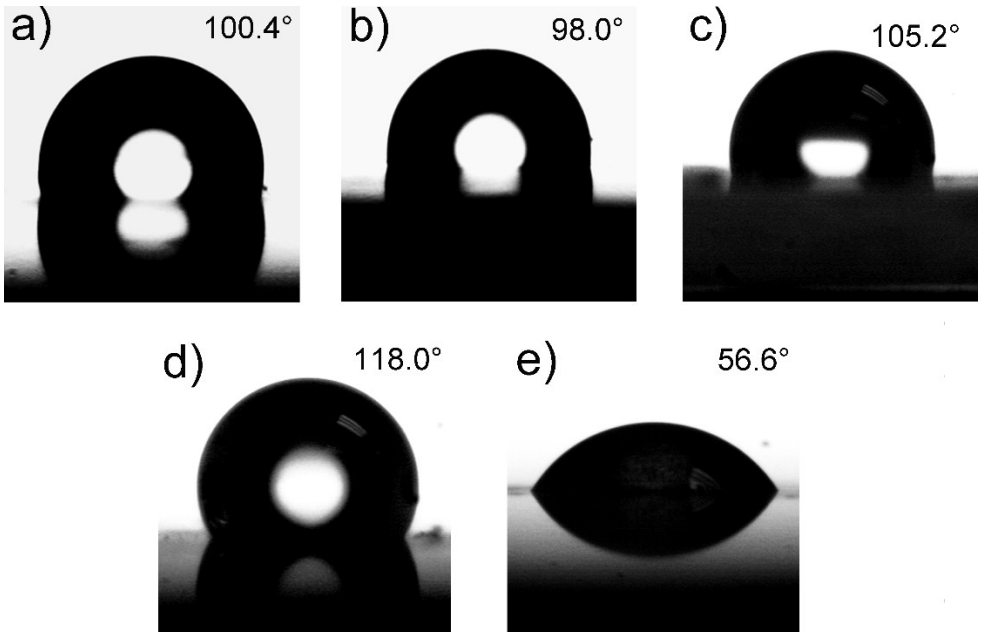

Figure S24. Water contact angle (WCA) of CMP nanofilms. a) CMP-1-nanofilm. b) CMP-2-nanofilm. c) CMP-3-nanofilm. d) CMP-4-nanofilm. e) Imine-CMP-nanofilm .

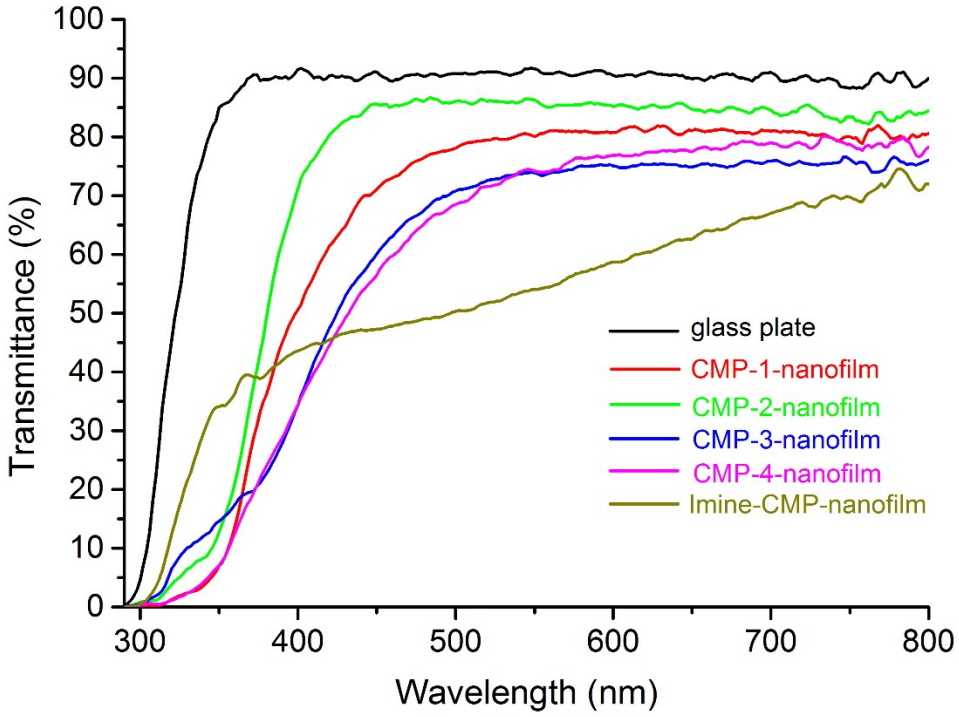

Figure S25. UV–Vis transmission spectra of CMP nanofilms and bare glass plate.

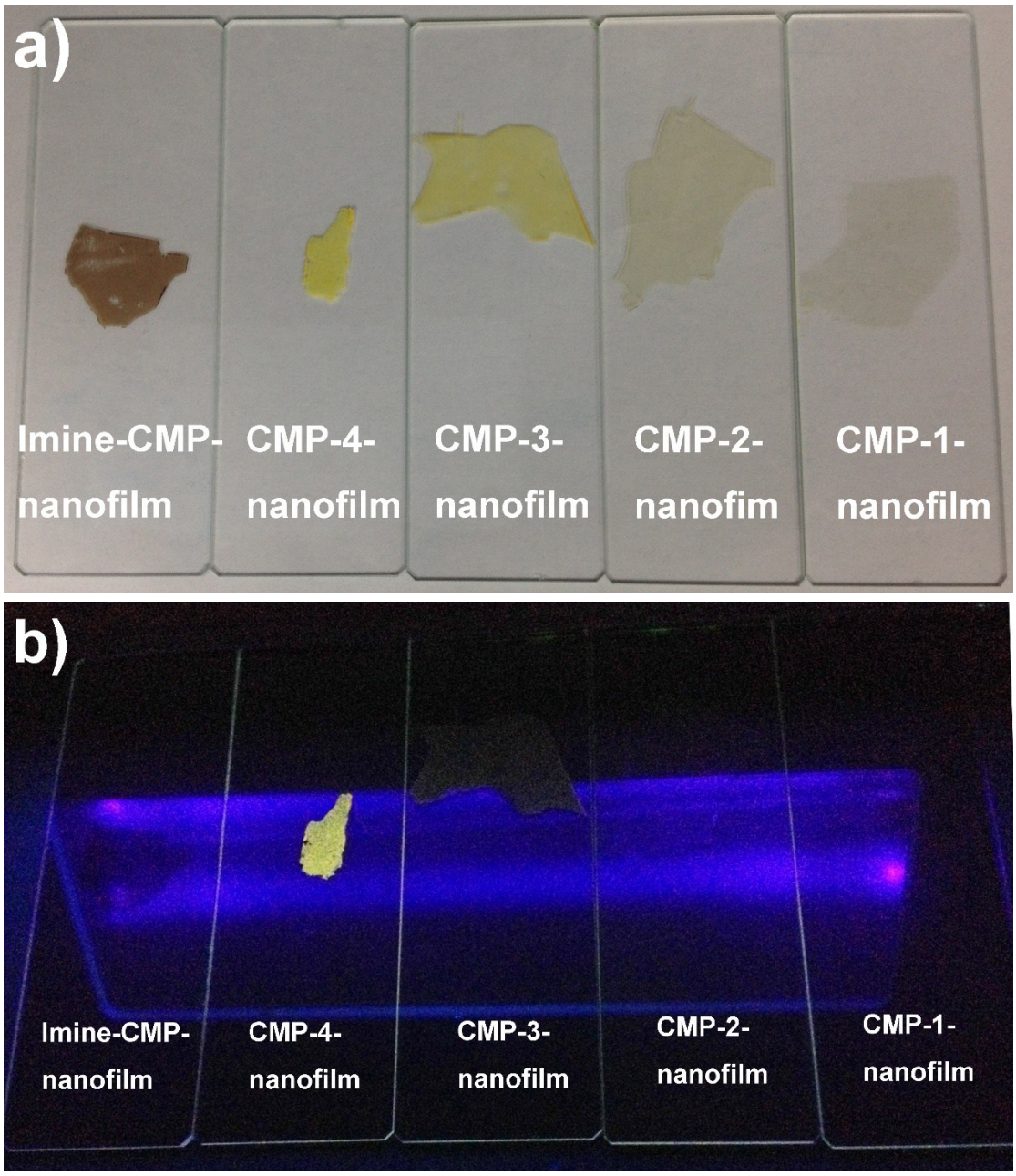

Figure S26. a) Photo images of nanofilms on quartz plates. b) The corresponding photo images of a) under hand-held UV lamp at 254 nm.

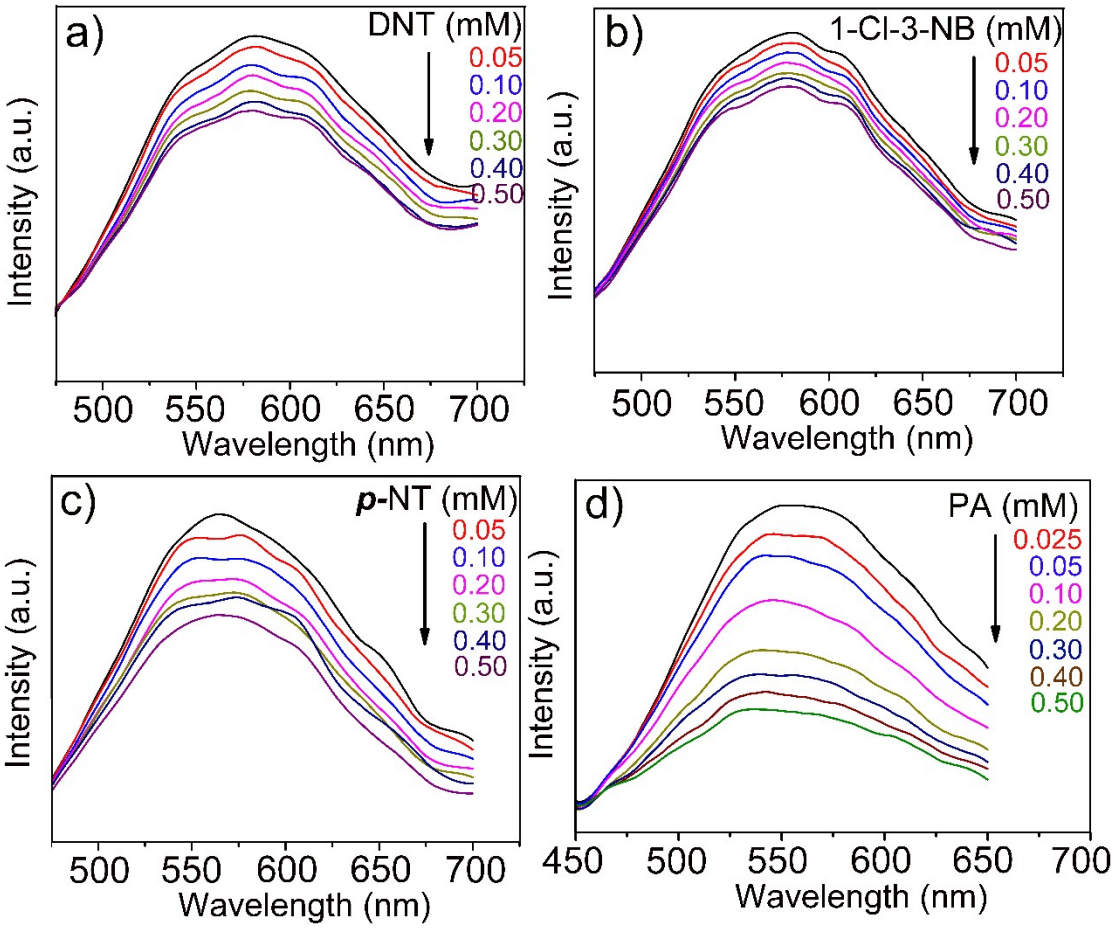

Figure S27. a-c) Corrected emission spectra illustrate the fluorescence quenching of CMP-4-nanofilm (thickness is around 180nm) with increasing nitroaromatics concentrations, a) DNT, b) 1-Cl-3-NB, c) ***p***-NT. d) Fluorescence quenching of CMP-4-nanofilm (thickness is around 100nm) with increasing PA concentrations.

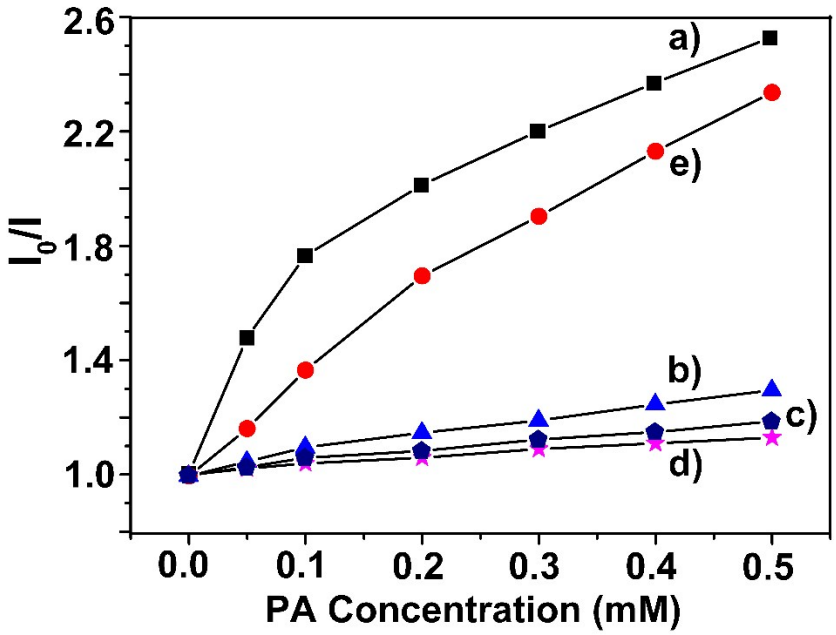

Figure S28. (a-d) The Stern-Volmer plots obtained from titration of the CMP-4-naofilms (thickness is around 180 nm) with nitroaromatics: a) PA, Ksv= 1.90×10^3 M^{-1}; b) ***p***-NT, Ksv= 0.53×10^3 M^{-1}; c) DNT, Ksv= 0.34×10^3 M^{-1}; d) 1-Cl-3-NB, Ksv= 0.24×10^3 M^{-1}. e) The Stern-Volmer plots obtained from titration of the CMP-4-naofilms (thickness is around 100 nm) with PA, Ksv= 2.38×10^3 M^{-1}.

Table S1. BET surface areas and pore diameters of CMP nanofilms and CMP bulk powders.

Polymer network	Nanofilm		Bulk powder	
	S_{BET} (m^2/g)[a]	Pore diameter (nm)[b]	S_{BET} (m^2/g)[a]	Pore diameter (nm)[b]
CMP-1	750	0.52	687	0.72
CMP-2	759	0.58	553	0.60
CMP-3	1038	1.80	685	0.51
CMP-4	680	1.40	236	0.61
Imine-CMP	22	1.30	17	3.30

[a] Surface areas of CMP nanofilms and CMP bulk powders calculated from Kr adsorption isotherm (77K) and N_2 adsorption isotherm (77K) using the Brunauer–Emmett–Teller method, respectively.

[b] Pore diameter corresponding to the maximum of the pore size distribution (DFT model).

Table S2. Comparison of quenching constant for explosives.

Materials	Synthesis methods	Solutions	Explosives	Quenching constant (M^{-1})
CMP-4-nanofilm (around 180 nm/ 100 nm) [**This work**]	Interfacial polymerization	Acetonitrile	PA	1.9×10^3/ 2.38×10^3
TPE-based conjugated polymer film[S2]	Spin-coating	Water	PA	1.8×10^3
PolyTPECz porous film[S3]	Electropolymerization	Acetonitrile	PA	6.4×10^4
Sn–porphyrin porous film[S4]	Synthesized on TLC plates	Water	PA	1.0×10^4
Tetraphenyl-5,5-dioctylcyclopentadiene(TPDC) based porous polymer nanoparticle [S5]		THF	PA	2.1×10^3
3D porous MOF[S6]		Acetonitrile	PA	3.5×10^4
Porous hyperbranched conjugated polymer nanoparticle [S7]		THF	TNT	1.38×10^3
2D porous covalent organic nanosheets[S8]	Solvothermal protocol	Isopropyl alcohol	PA	2.6×10^4
Dual-functional MOF[S9]		Ethanol	PA	7.34×10^4
Two luminescent Cd(II) MOF[S10]		DMF	PA	1.41×10^4

Supporting References

[S1] Jiang, J. X.; Su, F.; Trewin, A.; Wood, C. D.; Campbell, N. L.; Niu, H.; Dickinson, C.; Ganin, A. Y.; Rosseinsky, M. J.; Khimyak, Y. Z.; Cooper, A. I. Conjugated Microporous Poly(aryleneethynylene) Networks. *Angew. Chem., Int. Ed.* **2007**, *46,* 8574.

[S2] Xu, B.; Wu, X.; Li, H.; Tong, H.; Wang, L. Selective Detection of TNT and Picric Acid by Conjugated Polymer Film Sensors with Donor-Acceptor Architecture. *Macromolecules,* **2011**, *44,* 5089.

[S3] Gu, C.; Huang, N.; Wu, Y.; Xu, H.; Jiang, D. Design of Highly Photofunctional Porous Polymer Films with Controlled Thickness and Prominent Microporosity. *Angew. Chem., Int. Ed.* **2015**, *54*, 11540.

[S4] Ko, J. H.; Moon, J. H.; Kang, N.; Park, J. H.; Shin, H. W.; Park, N.; Kang, S.; Lee, S. M.; Kim, H. J.; Ahn, T. K.; Lee, J. Y.; Son, S. U. Engineering of Sn–Porphyrin Networks on The Silica Surface: Sensing of Nitrophenols in Water. *Chem. Commun.* **2015**, *51*, 8781.

[S5] Bandyopadhyay, S.; Pallavi, P.; Anil, A. G.; Patra, A. Fabrication of Porous Organic Polymers in the Form of Powder, Soluble in Organic Solvents and Nanoparticles: a Unique Platform for Gas Adsorption and Efficient Chemosensing. *Polym. Chem.,* **2015**, *6*, 3775.

[S6] Nagarkar, S. S.; Joarder, B.; Chaudhari, A. K.; Mukherjee, S.; Ghosh, S. K. Highly Selective Detection of Nitro Explosives by a Luminescent Metal–Organic Framework. *Angew. Chem., Int. Ed.* **2013**, *52*, 2881.

[S7] Wu, X.; Li, H.; Xu, B.; Tong, H.; Wang, L. Solution-dispersed Porous Hyperbranched Conjugated Polymer Nanoparticles for Fluorescent Sensing of TNT with Enhanced Sensitivity. *Polym. Chem.,* **2014**, *5,* 4521.

[S8] Das G.; Biswal B. P.; Kandambeth S.; Venkatesh V.; Kaur G.; Addicoat M.; Heine T.; Verma S.; Banerjee R. Chemical Sensing in Two Dimensional Porous Covalent Organic Nanosheets. *Chem. Sci.,* **2015**, *6*, 3931.

[S9] Wang K.M.; Du L.; Ma Y.L.; Zhao Q.H. Selective Sensing of 2,4,6-trinitrophenol and Detection of The Ultralow Temperature Based on a Dual-functional MOF As a Luminescent Sensor. *Inorg. Chem. Commun.,* **2016**, *68*, 45.

[S10] Wang Z.J.; Qin L.; Chen J.X.; Zheng H.G. H‑Bonding Interactions Induced Two Isostructural

Cd(II) Metal−Organic Frameworks Showing Different Selective Detection of Nitroaromatic Explosives *Inorg. Chem.,* **2016**, *55*, 10999.